The impact of multi-decadal changes in VOCs speciation on urban ozone chemistry: A case study in Birmingham, United Kingdom.

Jianghao Li[1,2], Alastair C. Lewis[1,3], Jim R. Hopkins[1,3], Stephen J. Andrews[1,3], Tim Murrells[4], Neil Passant[4], Ben Richmond[4], Siqi Hou[5], William J. Bloss[5], Roy M. Harrison[5,6], Zongbo Shi[5].

[1]Wolfson Atmospheric Chemistry Laboratories, University of York, York YO10 5DD, UK

[2]School of Water and Environment, Chang'an University, Xi'an 710064, China

[3]National Centre for Atmospheric Science, University of York, Heslington, York YO10 5DD, UK

[4]Ricardo Energy and Environment Gemini Building, Fermi Avenue, Harwell, Oxon OX11 0QR, UK

[5]School of Geography, Earth and Environmental Sciences, University of Birmingham, Edgbaston, Birmingham B15 2TT, UK

[6]Department of Environmental Sciences, Faculty of Meteorology, Environment and Arid Land Agriculture, King Abdulaziz University, P.O. Box 80208, Jeddah 21589, Saudi Arabia

Correspondence to: Jianghao Li (cfm531@york.ac.uk)

Abstract Anthropogenic non-methane volatile organic compounds (VOCs) in the United Kingdom have been substantially reduced since 1990, in part attributed to controls on evaporative and vehicle tailpipe emissions. Over time other sources with a different speciation, for example alcohols from solvent use and industry processes, have grown in both relative importance and in some cases in absolute terms. The impact of this change in speciation and the resulting photochemical reactivities of VOCs are evaluated using a photochemical box model constrained by observational data during a summertime ozone event (Birmingham, UK), and apportionment of sources based on the UK National Atmospheric Emission Inventory (NAEI) data over the period 1990-2019. Despite road transport sources representing only 3.3% of UK VOC emissions in 2019, it continued as the sector with the largest influence on local O_3 production rate ($P(O_3)$). Under case study conditions, the 96% reduction in road transport VOC emissions that has been achieved between 1990 – 2019 has likely reduced daytime $P(O_3)$ by ~1.67 ppbv h^{-1}. Further abatement of fuel fugitive emissions was modeled to have had less impact on $P(O_3)$ reduction than abatement of VOCs from industrial processes and solvent use. The long-term trend of increased emissions of ethanol and methanol have somewhat weakened the benefits of reducing road transport emissions, increasing $P(O_3)$ by ~0.19 ppbv h^{-1} in

the case study. Abatement of VOC emissions from multiple sources has been a notable technical and policy success in the UK but some future benefits (from an ozone perspective) of the phase out of internal combustion engine passenger cars may be offset if domestic and commercial solvent use of VOCs were to continue to increase.

1. Introduction

Elevated tropospheric ozone (O_3) has been a long-standing pollutant of concern in the rural and sub-urban environment and is now becoming more prevalent in urban centers as primary NO traffic emissions reduce (Sicard, 2021). As an important tropospheric oxidant and greenhouse gas (Kumar et al., 2021), exposure to O_3 also increases risks of mortality from respiratory diseases and adversely impacts on crop productivity (Lefohn et al., 2018). O_3 is mainly formed through photochemical reactions involving the oxidation of volatile organic compounds (VOCs) in the presence of nitrogen oxides (NO_x, NO_x=NO+NO_2) (Calvert et al., 2015). The release of VOCs arises from a wide range of activities, including unburned fuel or partially combusted products in exhaust, from solvents used in industry and numerous other diffuse domestic and commercial sources (He et al., 2019). Effective policies to mitigate ozone pollution rely on an accurate estimate of both emissions and speciation of O_3 precursors.

The challenge in reducing O_3 lies in its non-linear relationship with its precursors since individual VOCs have unique capacities for forming ozone. Decades of modelling studies have established regimes where reductions in NO_x or VOCs emissions would be preferentially beneficial to mitigate O_3 – so-called NO_x-limited or VOC-limited regimes (Ivatt et al., 2022; Seinfeld and Pandis, 2016). Abatement of VOCs sources is important in VOCs-limited areas since decreasing the emissions can effectively reduce the local O_3 production rate and help limit O_3 peak concentrations (Gaudel et al., 2020). The wide range of sources, including many that are diffuse and occur indoors, and differing photochemical reactivities further complicates O_3 reduction strategies. Different mixes of sources and speciation can lead to a need for localized policies. For example, short-chain alkanes and alkenes with high hydroxyl radical reactivity emitted from on-road transportation in China, have been reported as being responsible for 26% of national O_3 formation (Wu and Xie, 2017). A field observation study in Delhi, India reported that the O_3 production in that city was most sensitive to

monoaromatics, followed by monoterpenes and alkenes during a post-monsoon period in 2018 (Nelson et al., 2021). Another study at urban sites in Seoul, South Korea concluded that the O_3 production was controlled by C>6 aromatics and isoprene during a summer O_3 episode in 2016 (Schroeder et al., 2020). There is therefore no 'one size fits-all' policy in terms for which sources and sectors to target for optimal O_3 abatement efforts.

Policy and regulation aimed at improving air quality in many countries including the United States, the United Kingdom and Europe have led to decades of falling VOCs emissions (Lewis et al., 2020; Coggon et al., 2021). This reduction can be substantially attributed to the successful technical implementation of tailpipe exhaust after-treatment technology for gasoline vehicles controls on evaporative emissions from vehicles including during re-fueling and a more widespread set of efforts to control industrial emissions (Winkler et al., 2018). Despite these successes, O_3 remains a pollutant of concern; whilst peak concentrations during O_3 events have reduced in the UK, increases in the long-term urban background O_3 concentrations have been observed since the 1990s (Department for Environment, Food & Rural Affairs, 2023). A variety of explanations have been given to account for the increase including a rising northern hemisphere background O_3, increasing methane which contributes to both global radiative forcing and enhances O_3 production (Tarasick et al., 2019; Abernethy et al., 2021), the increases in non-vehicular sources of VOCs emissions (Mcdonald et al., 2018; Yeoman and Lewis, 2021), and the reduction of NO_x in VOCs-limited urban areas leading to greater O_3 production efficiency (Diaz et al., 2020).

The UK National Atmospheric Emissions Inventory (NAEI) for VOCs has shown increases in the relative contribution of solvent usage and the food & wine industry to total national VOCs emission over 1990-2019, and steady growth in the relative importance of OVOCs within the overall speciation (Lewis et al., 2020). In North America and Europe cities, OVOCs emitted from volatile chemical products (VCP) can outweigh fossil fuel sources for urban VOCs. Modelling results showed that the additional OVOCs from VCP emissions were the most important species for urban O_3 production, increasing the daily maximum O_3 mixing ratio by as much as 10 ppbv in Los Angeles and 11 ppbv in New York (Coggon et al., 2021; Qin et al., 2021). Substantial OVOCs emissions can come from unexpected places. For example, alcohols emitted from use of windshield fluid are now estimated to be a larger VOC source from road transport than VOC from the tailpipe in the UK (Cliff et al., 2023). From the perspective of O_3 pollution, the benefit of substantial reductions on

vehicle emissions, whilst there has been a parallel increasing role for non-industrial solvent usage remains unclear. What effect this shift in speciation is having on ozone chemistry is less well studied. One challenge has been the lack of routine measurement of OVOCs in most national air quality monitoring networks (Air Quality Expert Group, 2020).

In this study we evaluate the effects of changing speciation on urban ozone chemistry, using recent field measurements of O_3 and its key precursors such as NO_x, CO, speciated VOCs and OVOCs in Birmingham, UK during August 2022. We combine this with changing speciation and relative amounts of VOCs based on long-trends in the NAEI. The sensitivity of *in- situ* production and OH reactivities of the measured O_3 precursors are investigated by constraining the observational data sets to a zero-dimensional chemical box model. By incorporating the detailed NAEI VOCs emission inventories over the period of 1990-2019 into the model, O_3 formation in Birmingham is used as a case study to quantify the impacts of the real-world changes in VOCs sources on urban O_3 production rate. The relative importance of different VOCs functional group classes to O_3 production are also evaluated. The results help understand impacts of decades of abating different VOCs-emitting sectors on urban O_3 production, and outline the implications for future O_3 control strategies.

2. Materials and Methods

2.1 Field observations

The observations are taken from the Birmingham NERC Air Quality Supersite during August 2022. This is located on the University of Birmingham (52°27'20.2"N 1°55'44.3"W) campus. The site has been in operation for many years, and represents an urban background environment. It is influenced by transport emissions from nearby arterial roads and residential emissions from surrounding area. There are no significant industrial activities within a 4km radius of the site.

Continuous measurements of NO, NO_2, CO, CH_4, VOCs, O_3, along with meteorological parameters including air temperature and pressure, relative humidity, wind speed and direction were made. Briefly, NO and NO_2 were measured by a chemiluminescence-based T200 analyzer (Teledyne API., U.S.A.) and the T500U Cavity Attenuated Phase Shift (CAPS) analyzer (Teledyne API., U.S.A.). The concentration of NO_x was then the statistical sum of NO and NO_2. The mixing ratio of

CO were measured by a laser absorption spectroscopy Multi-species Continuous Emissions Monitoring instrument (Enviro Technology Service Ltd., UK) (Li et al., 2020). Manual calibration and span checks for the above instruments were performed every 3 days, and automatic zero calibration was set on daily bases. O_3 was measured by an O_3 analyzer (Model 49i, Thermo Fisher Scientific Inc., U.S.A.) with a minimum detection limit (MDL) of 1.0 ppbv. Meteorological parameters including air temperature and pressure, and relative humidity were obtained from a weather station WS300-UMB weather station (Luff GmbH, Germany). Additionally, Wind speed and direction were measured by a 3-axis ultrasonic anemometer (Gill Instruments Ltd., UK) over the campaign.

A gas chromatography-flame ionization detection (GC-FID) analysis system (7890A, Agilent Technologies, U.S.A.) was used to quantify 38 individual VOCs species. Details on instrument settings and quality assurance/quality control methods can be found in (Warburton et al., 2023). Briefly, the GC-FID system utilizes dual detectors: one detector for C_2 – C_6 non-methane hydrocarbons (NMHCs); the other detector for remaining C ≥ 7 hydrocarbons, and polar species such as ethers, ketones, and alcohols. Ambient samples were dried at −40 °C using a water trap and then preconcentrated on a carbon adsorbent at the lowest temperature the unit could achieve, always lower than -115 °C. Once a 0.5L sample had been collected, a pre-concentration trap was warmed slightly from -80 °C to purge trapped atmospheric CO_2. The trap was then heated to 190 °C for 3 minutes with a counter flow of helium thermally desorbing the concentrated VOCs onto focusing micro-trap held at lower than -115 °C. The analytes were flash heated and passed onto a VF-WAX column. The unresolved analytes (C_2 – C_6 NMHCs) were then transferred into a Na_2SO_4-deactivated Al_2O_3 porous-layer open tubular (PLOT) column via a Deans switch, for separation and detection by the first FID. The Dean switch then diverted the analytes onto a fused silica internal diameter to balance column flows and subsequently transfer the VF-WAX column- resolved species into the second FID. Generally, quantification of C_2-C_6 hydrocarbons was completed by the first FID using 4 ppbv gas standard cylinders (the National Physical Laboratory, Teddington, UK). Quantification of C ≥ 7 hydrocarbons and OVOCs was completed by the second FID using effective carbon number (ECN) with reference to toluene. In this study, the concentration of total VOC (TVOC) was defined as the statistical sum of concentrations of measured individual species, but this is not meant to infer that this represents the total reactive carbon in air, which would always be greater than this value

148 due to unmeasured species. Later in this study we broadly group species according to their chemical
149 function groups, summing into alcohols, ketones, alkanes, alkenes, aromatics, aldehydes, and
150 alkynes.

151 The GC-FID system responses were regularly checked by running direct calibration sequences
152 using the 4 ppbv gas standard cylinders. It was verified there was no FID-response drift over the
153 analyzing period for this study. Additionally, carbon-wise FID responses for all reported species
154 were calculated to verify the use of ECN as a quantification method. Table S1 lists which species
155 were directly calibrated, and which used equivalent carbon numbers for quantification. Table S2
156 shows effective carbon numbers of species which used carbon-wise responses.

157 ## 2.2 National emission inventory for VOCs

158 Estimates of UK anthropogenic VOC emissions are taken from the NAEI. The NAEI uses a
159 combination of UK-specific methods and default methods as recommended in the European
160 Monitoring and Evaluation Programme (EMEP)/European Environment Agency (EEA) Emission
161 Inventory Guidebook (European Environment Agency, 2016). Further details can be found in (NAEI,
162 2021). The VOC inventory is also disaggregated into inventories for each individual VOC species
163 and details of the speciation process and assumptions can be found in (Passant, 2002) and (Lewis et
164 al., 2020).

165 Methods to estimate emissions can be divided into two groups: those using emission factors,
166 and those using 'point source' emissions data reported to regulators by the operators of individual
167 industrial sites. The emission factor methods require UK activity data, for example consumption of
168 paint, consumption of a fuel, production of steel or vehicle kilometers travelled. The activity data is
169 then combined with an emission factor which expresses the total VOC emission that is expected per
170 unit of a given activity. Most total VOC emission factors are taken from the internationally applied
171 EMEP/EEA Emission Inventory Guidebook and so are not necessarily UK-specific. The factors for
172 road transport are directly calculated for the UK and a particularly detailed approach is used to
173 estimate emissions using emission factors from the Guidebook for many different vehicle types and
174 emission standards, fuels and road types combined with detailed transport activity from the UK
175 Department for Transport. Government statistics cannot always provide the necessary activity data
176 for other sectors, so industry data are used instead. For instance, NAEI data on consumption of
177 products containing organic solvents are from industry sources. The alternative point source method

can be used for source categories where emissions data can be obtained for all sites within the sector, and this limits the method to source categories such as crude oil refining, steel production and chemicals production. The emissions data reported by the operators of these sites can be based on emissions monitoring, although this is not always the case and emissions might instead be estimated, for example, using emission factors.

The NAEI produces updates to the inventory for total VOC mass emissions by source sector each year to achieve a consistent historic time-series reflecting trends in UK emissions. Emissions of individual VOC species are estimated using source-specific speciation profiles which show the mass fraction of each species, or in some cases groups of species, emitted by the source (NAEI, 2021; Passant, 2002). Over 600 individual VOC species or species groups are included in the speciation, based on sources in industry, regulators and in some cases literature sources and databases such as the USEPA SPECIATE database. The speciated inventory tends to be more uncertain than the estimation of total mass of VOC emissions. The inventory for total VOC mass is updated annually, whereas the speciation profiles are only periodically updated when new information becomes available. Thus, trends in a particular species for a sector are a reflection of changes in total VOC emissions for the sector and do not normally reflect any changes over time in the speciation profile of the sector which may have occurred.

2.3 Photochemical box model

The framework for evaluating effects of changing VOCs speciation is a 0-D Atmospheric Modelling chemistry box model (Wolfe et al., 2016), driven by the Version 3.3.1 of the Master Chemical Mechanism (MCM v3.3.1) (Saunders et al., 2003; Jenkin et al., 2003). The model can be effective in identifying the instantaneous *in- situ* O_3 sensitivity to changes in individual VOCs. The measured concentrations of 38 VOCs species, NO_x, and CO, along with air temperature and pressure, and relative humidity were averaged to a time resolution of 1-hour to constrain the model. A 3-day model spin-up, with each 24-hour model run constrained by the observational data, was performed in order to initialize the unmeasured compounds and transient radicals. The modelled outputs on the 4^{th} day were taken as representing steady state of the photochemistry.

Photolysis rates were calculated as a function of solar zenith angle (Saunders et al., 2003):

$$J = l(\cos\chi)^m \exp(-n\sec\chi) \quad (1)$$

Where J is the photolysis rate in s^{-1}; l, m, n are constants derived from radiative transfer model

runs for clear sky condition at an altitude of 0.5 km and literature cross sections/quantum yields; χ is the solar zenith angle in radians.

The net production rate of O_3 ($P(O_3)$) is calculated by the difference of the production rate of O_3 and the destruction rate of O_3, as in Equation (2):

$$P(O_3) = (k_{HO_2+NO}[HO_2][NO] + \sum_i k_{RO_{2_i}+NO}[RO_2][NO]) - (k_{O^1D+H_2O}[O^1D][H_2O] + k_{O_3+OH}[O_3][OH] + k_{O_3+HO_2}[O_3][HO_2] \quad (2)$$
$$k_{NO_2+OH}[NO_2][OH] + \sum_i k_{RO_{2_i}+NO_2}[RO_2][NO_2])$$

Where the former part is the rate of O_3 production, representing by rate of NO oxidation by HO_2 and RO_2 radicals; the latter part is the destruction rate of O_3, calculating by the sum of the rate of O_3 photolysis, the rates of the reactions with OH and HO_2 radicals, and the rates of NO_2 loss through reactions with OH and RO_2 radicals.

The sensitivity of O_3 to its precursors is quantified by the index of relative incremental reactivity (RIR) (Liu et al., 2022b), as in Equation (3):

$$RIR = \frac{\Delta P(O_3)}{P(O_3)} \times a^{-1} \quad (3)$$

Where RIR is the Relative Incremental Reactivity in %/%, $\Delta P(O_3)/P(O_3)$ is the ratio of the change in O_3 production rate to the base O_3 production rate; *a* is the reduction percentage in the input concentration of O_3 precursors – a factor that allows for the effects of changing absolute amounts of VOCs to be evaluated. Here a value of 30% was adopted for *a*.

3. Results and Discussion

3.1 Observation overview

The time series of O_3 and its precursors during August 2022 are shown in Figure 1, subdivided into periods that will be referred to as 'initial period', 'O_3 period', and 'clear–out'. The three periods covered 1st August-21th August 2022. Each period included one full week to avoid weekday/weekend differences in NO_x and VOCs concentrations impacting differently when O_3 production was compared between the three periods (de Foy et al., 2020). Ozone showed a generally increasing trend from 1st to 14th August and then returned to relatively low concentrations after 15th August 2022. The daily maximum 8 h average O_3 concentrations (MDA8h O_3) during the O_3 period exceeded the WHO guideline value (100 μg m^{-3}), ranging from 111 to 153 μg m^{-3}. The elevated O_3

during the middle of the month corresponded to more intense photochemical formation under hot weather conditions (32.7 °C in maximum) and higher concentrations of O_3 precursors (Table S3).

The diurnal profile of NO and NO_2 in the three periods generally showed a bimodal pattern, albeit less pronounced in the initial and clear–out periods (Figure 2). The two peaks likely arise as a consequence of increased traffic volumes at the start and end of the day, coupled to boundary layer height changes in the early morning and into the evening (Lee et al., 2020). The average concentrations of NO_2 during 05:00-10:00 were 10.8 ppbv in the O_3 period, which was considerably higher than the concentration of 3.9 ppbv in the initial period and 3.4 ppbv in the clear–out period. The low level of NO in the O_3 period highlights the rapid consumption of NO via photochemical processes. The oxidation of CO is an important source of HO_2 in the atmosphere (Chen et al., 2020), here in the range of 82.5 to 134.2 ppbv with little difference between periods. The diurnal profiles of O_3 peaked at 15:00, with maximum hourly concentrations of 31.6, 67.2, and 30.4 ppbv in the initial, O_3, and clear–out periods, respectively. Slight decreases in O_3 were observed during nighttime (00:00-05:00), indicating enhanced NO titration effects.

The detailed VOCs composition in the three periods is presented in Figure S1. Concentration of TVOC were 19.4 ± 8.4, 48.0 ± 18.8, and 23.5 ± 12.5 μg m^{-3} in the three periods, respectively. Alcohols, represented mainly by methanol and ethanol, were the predominant group that contributed 40.3% - 47.4% of over measured VOCs mass. This was followed by alkanes (21.4%-24.6%) and ketones (16.3%-17.3%). Contributions of aldehyde (acetaldehyde), aromatics, alkenes, and acetylene were low, ranging from 1.0% to 9.4% of total mass. Average mixing ratio of the top 10 species in selected periods at Birmingham Supersite are listed in Table S4. The top 10 species were represented by methanol, acetone, ethanol, acetaldehyde, and C_2 – C_4 alkanes across initial period, O_3 period, and clear-out period. The top individual species contributing to the total VOCs were methanol (10.3% – 33.6%) and acetone (15.5% – 17.1%), regardless of the subdivided periods. The results highlight large emissions of ethane, propane, n-butane, and i-butane associated with Natural Gas (NG), Liquefied Petroleum Gas (LPG), and propellant use, fuel combustion and evaporation. Ambient VOCs largely influenced by combustion-related sources (i.e., vehicle exhaust and coal combustion) generally show alkane-dominated composition (Wu and Xie, 2017). Here, the composition and amount of VOCs observed were most likely influenced by non-combustion processes such as volatile chemical product usage and industrial processes (Gkatzelis et al., 2020).

Methanol was the most abundant VOC with an average concentration of 4.1 ppbv, followed by acetone (2.0 ppbv), ethane (1.9 ppbv), ethanol (1.8 ppbv), and acetaldehyde (1.0 ppbv). The average ratio of ethene/ethane was 0.2 ± 0.1 over the campaign, considerably lower than seen in polluted locations, e.g. Hong Kong (China) (0.7 ± 0.1) (Wang et al., 2018) and Seremban (Malaysia) (1.1) (Zulkifli et al., 2022).

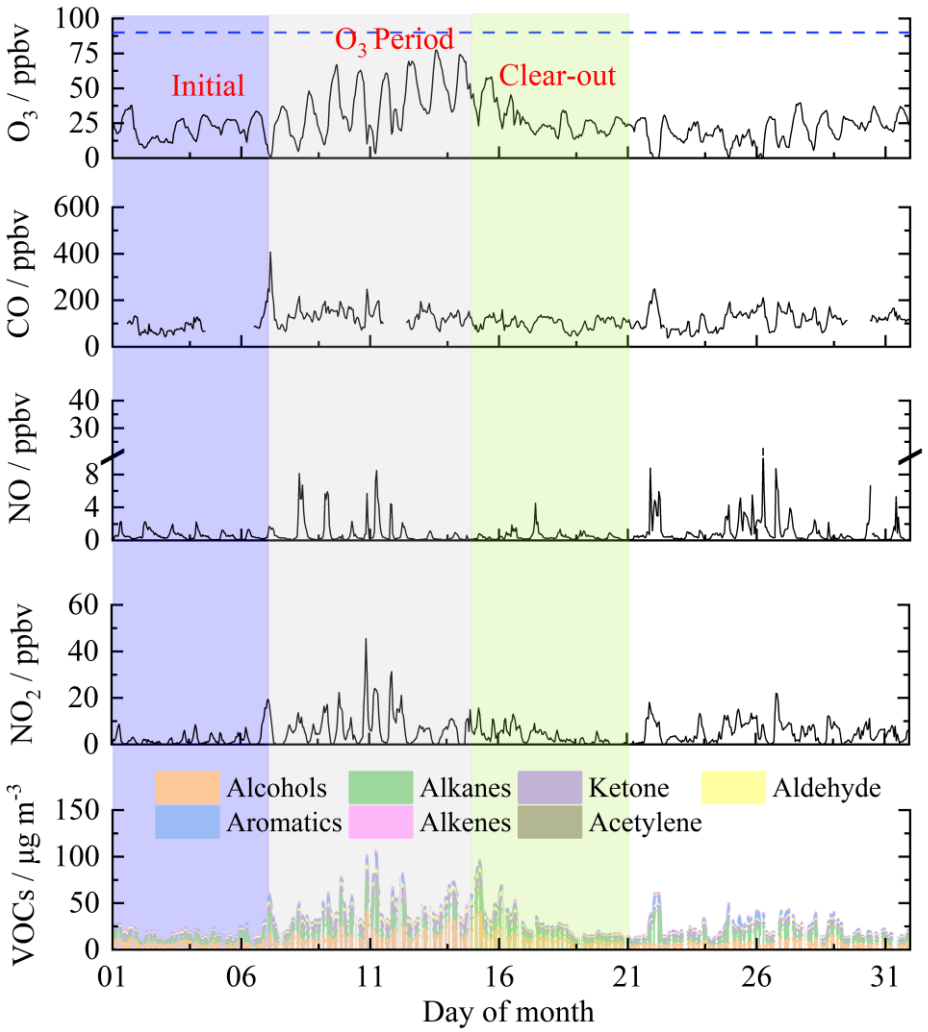

Figure 1. Time series of O_3, CO, NO, NO_2, and VOCs groups at the Birmingham Supersite. The blue dash line denotes the national standard (90 ppbv) for hourly O_3 concentration.

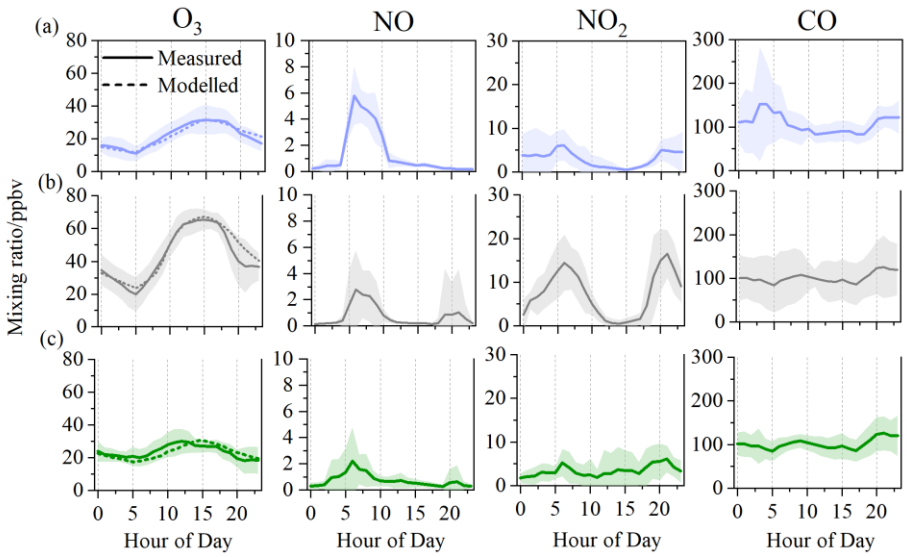

Figure 2. Diurnal variations of O_3, NO, NO_2, and CO during the initial (a), O_3 period (b), and clear–out period (c). The shaded areas represent standard variations.

The general diel profiles for all selected VOCs, except for ethane, showed bimodal pattern (Figure S2). Concentrations were much higher during the night, and lower in the day, due to they were subject to photochemical losses during the daytime. The bimodal pattern is less apparent for methanol and acetone, as they are abundant species originating from many anthropogenic sources in urban areas. For example, methanol was the most abundant species measured at a roadside in UK using Thermal Desorption-Gas Chromatography coupled with Flame Ionization Detection (TD-GC-FID) (Cliff et al., 2023). A separate study on gasoline and diesel vehicle exhausts reported methanol and acetone were the largest OVOCs emitted (Wang et al., 2022). Gkatzelis et al. (2021) conducted Positive Matrix factorization (PMF) analysis based on observed VOCs dataset in New York City, and concluded that acetone was the second most abundant species in measurements and was mostly attributed to volatile consumer product emissions (90%). (See Section 3.3 for further discussions for anthropogenic sources of OVOCs).

3.2 Observation-based O_3 formation sensitivity

The *in -situ* O_3 formation sensitivity was examined via reaction rates of ozone precursors and OH radical (OH reactivities, (k(OH))) and RIR scales of ozone precursors, along with the chemical budgets of O_3 formation and loss. In initial and clear-out periods. k(OH) exhibited consistent diurnal patterns, ranging from 2.4 to 5.9 s^{-1} (Figure S3). In the O_3 period, k(OH) reached 9.0 and 8.7 s^{-1} at approximately 07:00 and 20:00, respectively. A rapid increase in k(OH) was observed in the early

morning (00:00-06:00). VOCs and model generated species represented 60.5%, 65.7%, and 56.7% of the total *k*(OH) in the three periods, respectively. NO_x and CO only contributed 10.2% -27.9% to total *k*(OH). Among of the VOCs groups, alcohols exhibited the largest *k*(OH) in all periods, accounting for 5.0% - 6.9% of the total *k*(OH). The diurnal production and loss of O_3 are shown in Figure S4. The oxidation and photolysis of VOCs promoted the production of RO_2, and $NO+RO_2$ contributed 47.7% of the O_3 production pathways in the O_3 period and 36.2% and 39.8% in initial and clear–out periods, respectively. Considering O_3 destruction, $OH+NO_2$ was the most important pathway during morning (08:00-12:00), accounting for 73.5%, 55.4% and 59.4% of the O_3 destruction pathways in the three periods. The dominant $OH+NO_2$ contribution to O_3 destruction suggested that the *in -situ* O_3 productions in all three periods was sensitive to VOCs emissions to some extent.

In order to understand contributions of O_3 formation from direct emissions and secondary formations of OVOCs, we developed two modelling scenarios: (1) all OVOCs species were constrained to observed mixing ratio; (2) all OVOCs species were unconstrained. (2) allowed secondary formations of OVOCs by oxidations of their precursor VOCs. As shown in Figure S5, secondary formations of OVOCs had little impact on O_3 formation in all periods. The simulation of O_3 production using the box model without constraining observed OVOCs slightly underestimated average daily maximum O_3 mixing ratio and $P(O_3)$, compared to the scenario with all observed OVOCs species constrained. The underestimation for average daily maximum mixing ratio of O_3 was 4.8%, 6.9%, and 5.1% in initial period, O_3 period, and clear-out period, respectively. In this case, the underestimation of average daily maximum $P(O_3)$ was 5.1%, 6.0%, and 9.3% in the three periods, respectively. The results demonstrated that in the Birmingham case study, primary emissions of OVOCs played central role in the *in -situ* ozone production.

The relative incremental reactivity of NO_x, CO, and anthropogenic VOCs (AVOCs, all measured VOCs except for isoprene) are shown in Figure 3. The *in -situ* O_3 production was most sensitive to anthropogenic VOCs with the highest positive RIR values (0.44 - 0.49). This is as anticipated given earlier analyses demonstrating their role in determining *k*(OH) and O_3 production. The low RIR (0.03 - 0.07) for CO in all three periods indicated a minor contribution of CO oxidation to O_3 production. The high RIR (0.24) for NO_x was only observed in the O_3 period. Acetaldehyde showed the highest positive RIR (0.17 - 0.19) among the AVOCs, suggesting that the photolysis and

oxidation of acetaldehyde was a limiting factor for O_3 formation. The important role of carbonyl compounds in atmospheric photochemistry has also been reported in previous studies, contributing up to 59.3% to the O_3 formation in ambient environments in China, the United States, and Brazil (Qin et al., 2021; Liu et al., 2022a; Edwards et al., 2014). Alkanes and alcohols exhibited lower RIR values (0.02 - 0.04), despite their high mass concentrations.

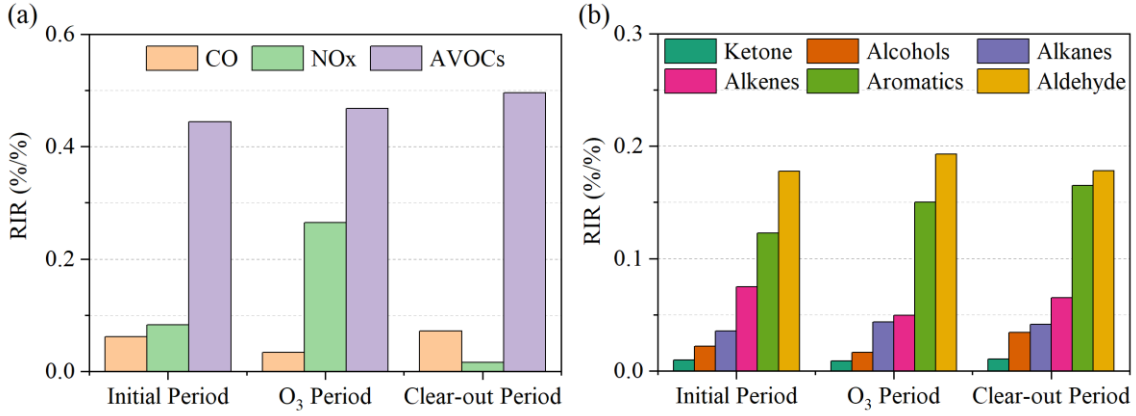

Figure 3. Modelled RIRs for (a) major O_3 precursors and (b) the AVOCs groups during photochemically active daytime (08:00-16:00) in the selected periods. (AVOCs: anthropogenic VOCs, all measured VOCs except for isoprene)

3.3 Emission inventory-informed O_3 production sensitivity tests

The trends in anthropogenic VOCs emissions from 1990 to 2019 estimated by the NAEI are shown in Figure S6. Over the period, the annual national emissions decreased by ~69.0% from 2,941 kt in 1990 to 911kt in 2019. The reduction is partly attributed to more stringent controls for gasoline vehicle emissions, both tailpipe and evaporative/fugitive. In 2019, VOCs emissions from on-road transport and fuel fugitive losses accounted for only 3.3% and 13.7% of the total mass of VOCs emissions, compared to 29.1% and 26.9% in 1990. Efforts have also been directed towards controlling industrial processes, commercial solvent usage, and combustion emissions, resulting in reductions of 66.8%, 48.9%, and 20.7%, respectively over the period. However, contributions from solvent usage to total VOCs emissions over 1990-2019 showed only modest reductions in the 1990s and 2000s and indeed small increases in the most recent years (Figure 4(b)). This slight growth in solvent usage is due to increasing emissions from solvent use in consumer products such as decorative products, aerosols, personal-care products, and detergents (NAEI, 2021). Solvent usage had become the largest contributory sector (33.7%) to VOCs emissions by 2019, followed by

industrial processes (16.0%).

As shown in Figure 4(a), the VOC speciation over the 1990-2019 period was dominated in mass terms by contributions from alkanes and alcohols, the former decreasing as gasoline sources declined, the other increasing as non-industrial solvent and food and drink industry processes emissions followed a different pattern. Alkane emissions fell from 46.6% to 30.6% over the period. Further reductions in alkane emissions are expected from policies for that phase-out sales of new internal combustion engine vehicles in the UK (and in many other places) by 2035. Growth in the relative contributions of alcohols was primarily driven by increases in emissions of methanol and ethanol, and to a lesser extent in 1-butanol and 2-propanol (Figure 4(c)).

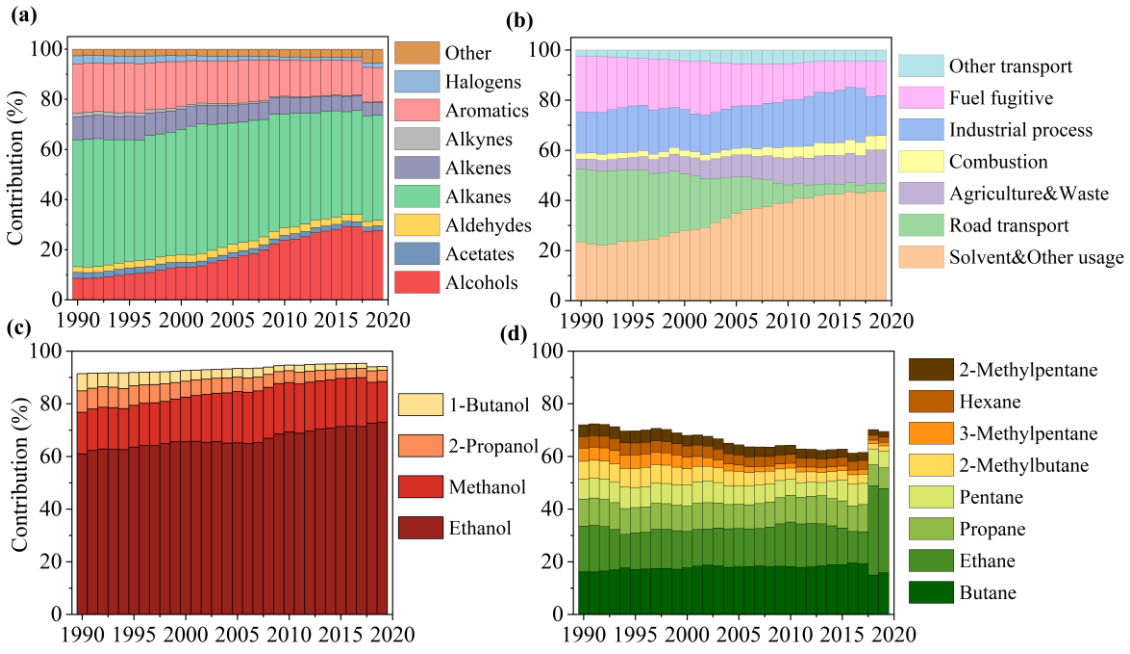

Figure 4. Contributions to annual national UK emissions of VOCs between 1990-2019 by: (a) functional group; (b) by major emissions reporting sector; (c) for four individual alcohols in the overall sub-class of alcohols; (d) for eight individual alkanes in the sub-class of all alkanes.

Figure S7 shows UK emission trends of individual species from different VOCs classes. These highlight a national trend since 1990 of decreasing emissions of ethane associated with natural gas leakage, toluene and propane associated with on-road petrol evaporation, as well as reductions of benzene, ethene, and acetylene associated with tailpipe exhaust. Meanwhile, the reduced emissions have been accompanied with increases in emissions of methanol and ethanol. The increase in methanol is largely attributed to increased emissions from car-care products (i.e., non-aerosol

products). The increase in ethanol is due to increased domestic and industrial solvent usage.

The NO_x, CO, and VOC speciation within the NAEI for each of the six major emission sectors was used to assign proportional sectoral contributions to the VOCs observed in Birmingham, and hence to ozone production in the case study. (Table S5). The six sectors are: road transport (both of on-road exhaust emission and evaporative losses of fuel vapor), industrial processes, combustion, solvent usage, fuel fugitive, and agriculture emissions). This makes a key assumption that the VOCs at the observation site are affected directly in the same proportion that VOCs are reported in national amounts in the NAEI. We make this assumption since it provides a reasonable starting point for understanding how each VOC sector may influence O_3 production during a case study event, however ozone formation might be sensitive to differing regional distribution in speciation. The attribution of VOCs sources based on the NAEI data can be thought of as representative for this case study as a typical urban environment, but it might not hold for cities near large industrial VOC sources (i.e., oil refinery and industrial production sites), since they can significantly affect composition and chemical reactivity of ambient VOCs.

Figure S8 shows the modelled RIRs for these sources in the initial, O_3, and clear–out periods. All the sources generally showed higher RIR values in the O_3 period. Road transport exhibited the highest positive RIR values in all periods (0.30 - 0.36), followed by industrial process (0.06 - 0.09) and solvent usage (0.05 - 0.07). Despite being a relatively minor contributor to the mass of national VOCs emissions (only 3.3% of the total in 2019), road transport VOCs still played the most important role in local ozone photochemical chemistry, in this case study.

Figure 5a shows the changes in $P(O_3)$ during the O_3 period from 08:00 to 16:00 which might arise as a result of reductions in the individual sectors described above. This is a 'thought experiment' where under 2019 general observed atmospheric conditions (e.g., for NO_x, CO and so on), each of the VOC source sectors is then further reduced in isolation (from 2019 levels) and the effects on $\Delta P(O_3)$ were evaluated. Based on these scenarios, reducing emissions from the individual sectors all resulted in decreased $P(O_3)$, as would be anticipated. Reducing ozone precursors arising from road transport would lead to a decreased $P(O_3)$ of ~1.71 ppbv h^{-1} if that sector could be 100% abated in the case study. This is expected because road transport is a source of photochemically reactive VOCs, including aromatics, aldehyde, and short-chain alkanes/alkenes. Other sectors showed more modest effects, with reductions in solvent-related VOCs the next most significant lever to control

ozone. Fully abating emissions of all industrial and solvent process emissions only resulted in a decreased $P(O_3)$ of ~0.35 ppbv h^{-1}, largely because they are dominated by ethanol and methanol with relatively low RIR values. Considering the real-world changes in VOC emissions over the period of 1990 to 2019, the very major reductions in road transport emissions have led to the largest effects in reducing $P(O_3)$ (Figure 5(b)). Whilst there have also been some very large reductions (94.6%) in fuel fugitive emissions, the impact on $P(O_3)$ reduction is modelled to have been relatively modest, being similar to industrial processes and solvent usage.

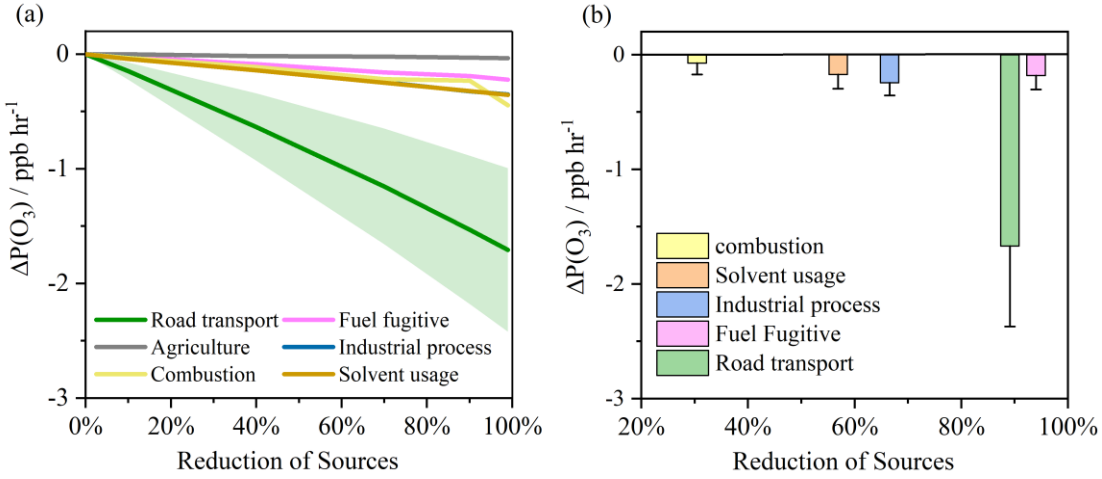

Figure 5. (a) Changes in $P(O_3)$ in response to different reductions in VOCs, NO_x, and CO from different sectors for the Birmingham-case study condition. (b) Changes in $P(O_3)$ based on the NAEI estimated reductions in VOCs from different sectors between 1990 and 2019. The standard deviations represent variability in $\Delta P(O_3)$ during 08:00-16:00 LST in the O_3 period.

Further model runs were performed to better understand the impacts of the shift between alkanes and alcohol species on $P(O_3)$, given trends showing decreasing alkanes emissions and increasing alcohol emissions between the 1990-2019 period (Figure 4). The modelled alkane concentrations in the case study were reduced by 10%, 30%, 50%, 70%, 90%, and 99%. This represents a downward trajectory in alkane emissions that would be anticipated as gasoline vehicles are slowly retired. Two further scenarios were then developed to sit alongside these reductions in alkanes. Firstly, the concentration of ethanol was increased to keep the overall total VOC concentrations in the model under case study conditions unchanged. Second, the concentration of both ethanol and methanol were scaled upwards to keep total VOCs concentration unchanged. As shown in Figure 6, reductions in alkanes alone resulted in decreased $P(O_3)$ to a maximum of ~0.26

ppbv h^{-1} if fully abated. If that alkane reduction was balanced with increased ethanol and methanol, then $\Delta P(O_3)$ is reduced by a maximum of 0.19 ppbv h^{-1}. If alkane reductions were balanced by increasing ethanol alone, then $P(O_3)$ still decreases, but only up to 0.07 ppbv h^{-1}.

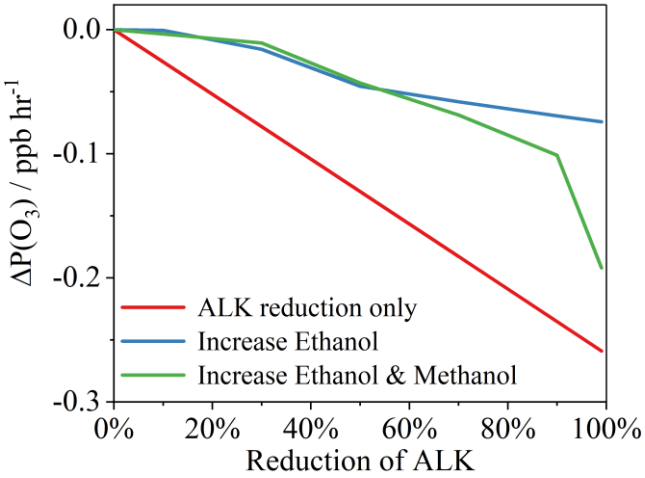

Figure 6. Reductions in $\Delta P(O_3)$ based on reducing alkanes (ALK) in the model (under case study conditions), reducing alkanes but balancing the overall VOC amount with increased ethanol (blue line) and reducing alkanes but balancing the overall VOC amount with increased ethanol and methanol (green line).

Conclusion

In this study a typical high-O_3 event in Birmingham, United Kingdom was chosen as a case study to investigate the impacts of changes to VOCs emissions and speciation on urban O_3 production. The *in- situ* O_3 formation sensitivity was split into three periods: initial, high O_3, and clear–out. Results from OH reactivity, O_3 budgets, and RIR index showed that O_3 formation in all three periods was impacted by both VOCs and NO_x, but was more sensitive to anthropogenic VOCs. The oxidation of alcohols and photolysis of acetaldehyde substantially contributed to *in- situ* O_3 formation, especially in the high O_3 period. The roles of anthropogenic VOC sources in urban O_3 chemistry were examined by integrating the NAEI speciation over the period of 1990-2019 into photochemical box model scenarios. Despite road transport only contributing 3.3% of national VOCs emissions in 2019 it still played the most important VOC role in the case study ozone photochemistry, when inventory contributions were mapped onto observed VOCs. Sequentially the observed VOCs were reduced by the fractional contributions and speciation in the NAEI for six

sectors to evaluate what impact abating different VOCs-emitting sectors would have on $P(O_3)$. Abating road transport VOCs in isolation would lead to a decreased $P(O_3)$ by up to 1.67 ppbv h^{-1}, but abating other sectors such as solvent use and fugitive fuels had noticeably smaller effects. Despite emissions of VOCs from road transport falling very dramatically between 1990 and 2019, it remains one of the most powerful means to further reduce ozone in this typical UK case study. The wider shift in speciation reported in the NAEI from alkanes to alcohols was also examined using scenarios where emission reductions for alkanes, were counterbalanced with increases in alcohols, all simulated for the Birmingham case study conditions (e.g., for NO_x, CO and etc). Further reducing alkanes from present day conditions to zero has a clear beneficial effect on reducing $P(O_3)$ by up to ~0.26 ppb hr^{-1}. However, this benefit would to a degree be offset should alcohol emissions (for example from food and drink, and/or solvent use) increase to counterbalance those alkanes reductions. Whilst simple alcohols are inherently less potent ozone-forming VOCs compared to the mixture of VOCs from road transport, avoiding future growth in emissions remains important, since they weaken the long-term benefits of road transport electrification and the phase out of internal combustion engine vehicles.

Data Availability

Observational data including meteorological parameters and air pollutants used in this study are available at https://github.com/nervouslee/Birmingham_CS.git. UK national emission inventory is available at https://naei.beis.gov.uk/.

Author Contribution

Jianghao Li prepared the manuscript with contributions from all authors. Alastair C. Lewis helped with modelling scenarios and revised the manuscript. Jim R. Hopkins contributed to measurement of chemical species. Stephen J. Andrews contributed to scientific discussion on findings of this work. Tim Murrells, Neil Passant and Ben Richmond contributed to the data of national emission inventory data and revision on NAEI methodology. Siqi Hou, William J. Bloss, Roy M. Harrison, and Zongbo Shi provided measurements of atmospheric pollutants used in this study, along with critical discussion on revising the manuscript.

Competing interests

The authors declare that they have no conflict of interest.

Acknowledgements

Establishment and operation of the Birmingham Air Quality Supersite operation (BAQS) is supported by the NERC WM-Air project (NE/S003487/1) and UKRI Clean Air SPF project OSCA (NE/T001976/1). This work forms part of the National Centre for Atmospheric Science National Capability programme funded by NERC. Jianghao Li's study at University of York is financially supported by the China Scholarship Council.

References

Abernethy, S., O'Connor, F., Jones, C., and Jackson, R.: Methane removal and the proportional reductions in surface temperature and ozone, Philosophical Transactions of the Royal Society A, 379, 20210104, 10.1098/rsta.2021.0104, 2021.

Air Quality Expert Group, Non-methane Volatile Organic Compounds in the UK: https://uk-air.defra.gov.uk/library/reports.php?report_id=10032020, last access: 07 September 2023.

Calvert, J. G., Orlando, J. J., Stockwell, W. R., and Wallington, T. J.: The mechanisms of reactions influencing atmospheric ozone, Oxford University Press, USA, 2015.

Chen, T., Xue, L., Zheng, P., Zhang, Y., Liu, Y., Sun, J., Han, G., Li, H., Zhang, X., and Li, Y.: Volatile organic compounds and ozone air pollution in an oil production region in northern China, Atmospheric Chemistry and Physics, 20, 7069-7086, 10.5194/acp-20-7069-2020, 2020.

Cliff, S. J., Lewis, A. C., Shaw, M. D., Lee, J. D., Flynn, M., Andrews, S. J., Hopkins, J. R., Purvis, R. M., and Yeoman, A. M.: Unreported VOC emissions from road transport including from electric vehicles, Environmental Science & Technology, 10.1021/acs.est.3c00845, 2023.

Coggon, M. M., Gkatzelis, G. I., McDonald, B. C., Gilman, J. B., Schwantes, R. H., Abuhassan, N., Aikin, K. C., Arend, M. F., Berkoff, T. A., Brown, S. S., Campos, T. L., Dickerson, R. R., Gronoff, G., Hurley, J. F., Isaacman-VanWertz, G., Koss, A. R., Li, M., McKeen, S. A., Moshary, F., Peischl, J., Pospisilova, V., Ren, X., Wilson, A., Wu, Y., Trainer, M., and Warneke, C.: Volatile chemical product emissions enhance ozone and modulate urban chemistry, Proc Natl Acad Sci U S A, 118, 10.1073/pnas.2026653118, 2021.

de Foy, B., Brune, W. H., and Schauer, J. J.: Changes in ozone photochemical regime in Fresno, California from 1994 to 2018 deduced from changes in the weekend effect, Environmental Pollution, 263, 114380, 10.1016/j.envpol.2020.114380, 2020.

Department for Environment, Food & Rural Affairs. An annual update of data on concentrations of major air pollutants in the UK: https://www.gov.uk/government/statistical-data-sets/env02-air-quality-

511 statistics, last access: 07 September 2023.
512 Diaz, F. M., Khan, M. A. H., Shallcross, B. M., Shallcross, E. D., Vogt, U., and Shallcross, D. E.: Ozone
513 trends in the United Kingdom over the last 30 years, Atmosphere, 11, 534, 10.3390/atmos11050534,
514 2020.
515 Edwards, P. M., Brown, S. S., Roberts, J. M., Ahmadov, R., Banta, R. M., deGouw, J. A., Dube, W. P.,
516 Field, R. A., Flynn, J. H., Gilman, J. B., Graus, M., Helmig, D., Koss, A., Langford, A. O., Lefer, B.
517 L., Lerner, B. M., Li, R., Li, S. M., McKeen, S. A., Murphy, S. M., Parrish, D. D., Senff, C. J., Soltis,
518 J., Stutz, J., Sweeney, C., Thompson, C. R., Trainer, M. K., Tsai, C., Veres, P. R., Washenfelder, R.
519 A., Warneke, C., Wild, R. J., Young, C. J., Yuan, B., and Zamora, R.: High winter ozone pollution
520 from carbonyl photolysis in an oil and gas basin, Nature, 514, 351-354, 10.1038/nature13767, 2014.
521 European Environment Agency.: EMEP/EEA air pollutant emission inventory guidebook 2016, 2016.
522 https://www.eea.europa.eu/publications/emep-eea-guidebook-2016, last access 07 September 2023.
523 Gaudel, A., Cooper, O. R., Chang, K.-L., Bourgeois, I., Ziemke, J. R., Strode, S. A., Oman, L. D., Sellitto,
524 P., Nédélec, P., Blot, R., Thouret, V., and Granier, C.: Aircraft observations since the 1990s reveal
525 increases of tropospheric ozone at multiple locations across the Northern Hemisphere, Science
526 Advances, 6, eaba8272, doi:10.1126/sciadv.aba8272, 2020.
527 Gkatzelis, G. I., Coggon, M. M., McDonald, B. C., Peischl, J., Aikin, K. C., Gilman, J. B., Trainer, M.,
528 and Warneke, C.: Identifying volatile chemical product tracer compounds in US cities,
529 Environmental Science & Technology, 55, 188-199, 10.1021/acs.est.0c05467, 2020.
530 He, Z., Wang, X., Ling, Z., Zhao, J., Guo, H., Shao, M., and Wang, Z.: Contributions of different
531 anthropogenic volatile organic compound sources to ozone formation at a receptor site in the Pearl
532 River Delta region and its policy implications, Atmospheric Chemistry and Physics, 19, 8801-8816,
533 10.5194/acp-19-8801-2019, 2019.
534 Ivatt, P. D., Evans, M. J., and Lewis, A. C.: Suppression of surface ozone by an aerosol-inhibited
535 photochemical ozone regime, Nature Geoscience, 15, 536-540, 2022.
536 Jenkin, M., Saunders, S., Wagner, V., and Pilling, M.: Protocol for the development of the Master
537 Chemical Mechanism, MCM v3 (Part B): tropospheric degradation of aromatic volatile organic
538 compounds, Atmospheric Chemistry and Physics, 3, 181-193, 10.5194/acp-3-181-2003, 2003.
539 Kumar, P., Kuttippurath, J., von der Gathen, P., Petropavlovskikh, I., Johnson, B., McClure-Begley, A.,
540 Cristofanelli, P., Bonasoni, P., Barlasina, M. E., and Sanchez, R.: The Increasing Surface Ozone and
541 Tropospheric Ozone in Antarctica and Their Possible Drivers, Environmental Science & Technology,
542 55, 8542-8553, 10.1021/acs.est.0c08491, 2021.
543 Lee, J. D., Drysdale, W. S., Finch, D. P., Wilde, S. E., and Palmer, P. I.: UK surface NO_2 levels dropped
544 by 42% during the COVID-19 lockdown: impact on surface O_3, Atmospheric Chemistry and Physics,
545 20, 15743-15759, 10.5194/acp-20-15743-2020, 2020.
546 Lefohn, A. S., Malley, C. S., Smith, L., Wells, B., Hazucha, M., Simon, H., Naik, V., Mills, G., Schultz,
547 M. G., Paoletti, E., De Marco, A., Xu, X., Zhang, L., Wang, T., Neufeld, H. S., Musselman, R. C.,
548 Tarasick, D., Brauer, M., Feng, Z., Tang, H., Kobayashi, K., Sicard, P., Solberg, S., and Gerosa, G.:
549 Tropospheric ozone assessment report: Global ozone metrics for climate change, human health, and
550 crop/ecosystem research, Elementa: Science of the Anthropocene, 6, 10.1525/elementa.279, 2018.
551 Lewis, A. C., Hopkins, J. R., Carslaw, D. C., Hamilton, J. F., Nelson, B. S., Stewart, G., Dernie, J.,
552 Passant, N., and Murrells, T.: An increasing role for solvent emissions and implications for future
553 measurements of volatile organic compounds, Philosophical Transactions of the Royal Society A,
554 378, 20190328, 10.1098/rsta.2019.0328, 2020.

Li, J., Yu, Z., Du, Z., Ji, Y., and Liu, C.: Standoff chemical detection using laser absorption spectroscopy: a review, Remote Sensing, 12, 2771, 10.3390/rs12172771, 2020.

Liu, Q., Gao, Y., Huang, W., Ling, Z., Wang, Z., and Wang, X.: Carbonyl compounds in the atmosphere: A review of abundance, source and their contributions to O_3 and SOA formation, Atmospheric Research, 106184, 10.1016/j.atmosres.2022.106184, 2022a.

Liu, T., Hong, Y., Li, M., Xu, L., Chen, J., Bian, Y., Yang, C., Dan, Y., Zhang, Y., and Xue, L.: Atmospheric oxidation capacity and ozone pollution mechanism in a coastal city of southeastern China: analysis of a typical photochemical episode by an observation-based model, Atmospheric Chemistry and Physics, 22, 2173-2190, 10.5194/acp-22-2173-2022, 2022b.

McDonald, B. C., De Gouw, J. A., Gilman, J. B., Jathar, S. H., Akherati, A., Cappa, C. D., Jimenez, J. L., Lee-Taylor, J., Hayes, P. L., and McKeen, S. A.: Volatile chemical products emerging as largest petrochemical source of urban organic emissions, Science, 359, 760-764, 10.1126/science.aaq0524, 2018.

National Atmospheric Emissions Inventory.: UK Informative Inventory Report (1990 to 2019), 2021. https://naei.beis.gov.uk/reports/reports?report_id=1016, last access 07 September 2023.

Nelson, B. S., Stewart, G. J., Drysdale, W. S., Newland, M. J., Vaughan, A. R., Dunmore, R. E., Edwards, P. M., Lewis, A. C., Hamilton, J. F., and Acton, W. J.: In situ ozone production is highly sensitive to volatile organic compounds in Delhi, India, Atmospheric Chemistry and Physics, 21, 13609-13630, 10.5194/acp-21-13609-2021, 2021.

Qin, M., Murphy, B. N., Isaacs, K. K., McDonald, B. C., Lu, Q., McKeen, S. A., Koval, L., Robinson, A. L., Efstathiou, C., and Allen, C.: Criteria pollutant impacts of volatile chemical products informed by near-field modelling, Nature sustainability, 4, 129-137, 10.1038/s41893-020-00614-1, 2021.

Saunders, S. M., Jenkin, M. E., Derwent, R., and Pilling, M.: Protocol for the development of the Master Chemical Mechanism, MCM v3 (Part A): tropospheric degradation of non-aromatic volatile organic compounds, Atmospheric Chemistry and Physics, 3, 161-180, 10.5194/acp-3-161-2003, 2003.

Schroeder, J. R., Crawford, J. H., Ahn, J.-Y., Chang, L., Fried, A., Walega, J., Weinheimer, A., Montzka, D. D., Hall, S. R., and Ullmann, K.: Observation-based modeling of ozone chemistry in the Seoul metropolitan area during the Korea-United States Air Quality Study (KORUS-AQ), Elementa: Science of the Anthropocene, 8, 3, 10.1525/elementa.400, 2020.

Seinfeld, J. H. and Pandis, S. N.: Atmospheric chemistry and physics: from air pollution to climate change, John Wiley & Sons, 2016.

Sicard, P.: Ground-level ozone over time: an observation-based global overview, Current Opinion in Environmental Science & Health, 19, 100226, 10.1016/j.eti.2022.102809, 2021.

Tarasick, D., Galbally, I. E., Cooper, O. R., Schultz, M. G., Ancellet, G., Leblanc, T., Wallington, T. J., Ziemke, J., Liu, X., and Steinbacher, M.: Tropospheric Ozone Assessment Report: Tropospheric ozone from 1877 to 2016, observed levels, trends and uncertainties, Elementa: Science of the Anthropocene, 7, 39, 10.1525/elementa.376, 2019.

Wang, S., Yuan, B., Wu, C., Wang, C., Li, T., He, X., Huangfu, Y., Qi, J., Li, X.-B., and Sha, Q. e.: Oxygenated volatile organic compounds (VOCs) as significant but varied contributors to VOC emissions from vehicles, Atmospheric Chemistry and Physics, 22, 9703-9720, 10.5194/acp-22-9703-2022, 2022.

Wang, Y., Guo, H., Zou, S., Lyu, X., Ling, Z., Cheng, H., and Zeren, Y.: Surface O_3 photochemistry over the South China Sea: Application of a near-explicit chemical mechanism box model, Environmental

Pollution, 234, 155-166, 10.1016/j.envpol.2017.11.001, 2018.
Warburton, T., Grange, S. K., Hopkins, J. R., Andrews, S. J., Lewis, A. C., Owen, N., Jordan, C., Adamson, G., and Xia, B.: The impact of plug-in fragrance diffusers on residential indoor VOC concentrations, Environmental Science: Processes & Impacts, 25, 805-817, 10.1039/D2EM00444E, 2023.
Winkler, S., Anderson, J., Garza, L., Ruona, W., Vogt, R., and Wallington, T.: Vehicle criteria pollutant (PM, NO_x, CO, HCs) emissions: how low should we go?, Npj Climate and atmospheric science, 1, 26, 10.1038/s41612-018-0037-5, 2018.
Wolfe, G. M., Marvin, M. R., Roberts, S. J., Travis, K. R., and Liao, J.: The framework for 0-D atmospheric modeling (F0AM) v3. 1, Geoscientific Model Development, 9, 3309-3319, 10.5194/gmd-9-3309-2016, 2016.
Wu, R. and Xie, S.: Spatial Distribution of Ozone Formation in China Derived from Emissions of Speciated Volatile Organic Compounds, Environmental Science & Technology, 51, 2574-2583, 10.1021/acs.est.6b03634, 2017.
Yeoman, A. M. and Lewis, A. C.: Global emissions of VOCs from compressed aerosol products, Elementa: Science of the Anthropocene, 9, 00177, 10.1525/elementa.2020.20.00177, 2021.
Zulkifli, M. F. H., Hawari, N. S. S. L., Latif, M. T., Abd Hamid, H. H., Mohtar, A. A. A., Idris, W. M. R. W., Mustaffa, N. I. H., and Juneng, L.: Volatile organic compounds and their contribution to ground-level ozone formation in a tropical urban environment, Chemosphere, 302, 134852, 10.1016/j.chemosphere.2022.134852, 2022.